

Subject: Ground-penetrating radar (GPR) and
electromagnetic induction (EM) investigations
within the Panola Mountain Research Watershed,
Stockbridge, Georgia; 4 to 9 June 1995.

Date: 7 July 1995

To: Dr. Jeff McDonnell
One Forestry Drive
State University of New York
College of Environmental Science and Forestry
Syracuse, New York 13210-2778

Purpose:

To evaluate the effectiveness of GPR and EM techniques for pedological investigations in a forested, topographically diverse, Piedmont terrain. Data will contribute to ongoing research projects assessing the suitability of the TOPMODEL hydrological model within the Panola Mountain Research Watershed.

Principal Participants:

Doug Burns, Graduate Student, SUNY, CESF, Syracuse, NY
Jim Doolittle, Research Soil Scientist, NRCS, Chester, PA
Janice McIntosh, Graduate Student, SUNY, CESF, Syracuse, NY
Al Zumbuhl, Graduate Student, SUNY, CESF, Syracuse, NY

Activities:

On 5 June, I arrived at the watershed, observed the research site, reviewed research activities, made survey plans, and prepared the equipment for field work. On 6 June, a survey of the research site was conducted with an EM38 meter. On 7 and 8 June, traverses using the SIR System-2 radar unit were conducted along selected transect lines, within a detailed grid site, and along trails within the watershed. Survey activities were completed on the morning of 9 June.

Panola Mountain Research Watershed

Panola Mountain Research Watershed is a 41 hectare catchment located within the Panola Mountain State Conservation Park in Rockdale County, north-central Georgia (Figure 1). The park is located about 25 kilometers southeast of Atlanta. The watershed is mostly forested. Large outcrops of Panola Granite are exposed on about 3 hectares of the catchment. Slopes are nearly level to steep. Relief is about 55 meters (Huntington et al., 1993).

The watershed is located within the Piedmont physiographic province. Soils formed principally in colluvium and residuum weathered from granite or gneiss bedrock. In many areas, the upper part of the bedrock has been decomposed by chemical weathering and layers of saprolite are present.

Within the watershed, soils have low base saturations and high proportions of kaolinite and gibbsite clays. The principal soils recognized within the research watershed include Altavista, Ashlar, Bibb, Cecil, Madison, Pacolet, Rion, Toccoa, and Wake. Altavista is a member of the fine-loamy, mixed, thermic Aquic Hapludults family. Ashlar is a member of the coarse-loamy, mixed, thermic Typic Dystrachrepts family. Bibb is a member of the coarse-loamy, siliceous, acid, thermic Typic Fluvaquents family. Cecil, Madison, and Pacolet are members of the clayey, kaolinitic, thermic Typic Kanhapludults family. Rion is a member of the fine-loamy, mixed, thermic Typic Hapludults family. Toccoa is a member of the coarse-loamy, mixed, nonacid, thermic Typic Udifluvents family. Wake is a member of the mixed, thermic Lithic Udipsamments family.

Soils depths are variable, but typically range from 0.6 to 1.6 m over saprolite or bedrock. Wake soils are shallow (< 50 cm), Ashlar and Madison soils are moderately deep (50 to 100 cm), Cecil soils are deep (100 to 150 cm), and Altavista, Bibb, Pacolet, Rion, and Toccoa are very deep (> 150 cm) to saprolite or bedrock.

Study Site

A 9.4 hectare portion of the catchment was selected for a detailed investigations. This study site is located in the extreme southwestern portion of the catchment.

The topography of the study site has been simulated in Figure 2. In Figure 2, the contour interval is 1.0 m. The coordinates are based on the Universal Transverse Mercator (UTM) grid system. These coordinates range from 761880 to 762200 (in Figure 2, 1880 to 2200) along the x axis, and from 3724180 to 3724560 (in Figure 2, 4200 to 4560) along the y axis.

The locations of a detailed grid site and several traverse lines are shown in Figure 2. The boundary of the study site conforms with summit slope positions and the boundary of the catchment. All portions of the study site slope towards a small drainageway which extends from its source in the southwest portion in a northeasterly direction across the site.

Table 1

Soil Map Units within The Study Site

<u>Soil Map Unit</u>	<u>Percent of Study Site</u>
Ashlar-Wake complex, 15-45 % slopes, very bouldery	58%
Madison sandy loam, 2-6 % slopes	14%
Madison sandy loam, 6-10 % slopes	3%
Rion sandy loam, 10-25 % slopes	14%
Rock outcrop	3%
Toccoa sandy loam, 0-3 % slopes, occasionally flooded	1%
Wake loamy coarse sand, 2-6 % slopes	7%

Table 1 list the dominant soil map units within the study site. Compared with other portions of the catchment, the study site is underlain by

bedrock at relatively shallower depths. Depths to bedrock or saprolite were characterized as being very shallow or shallow in 11 percent, shallow to moderately deep in 58 percent, moderately deep in 17 percent, and very deep in 14 percent of the study site.

MATERIALS AND METHODS

Equipment

The electromagnetic induction meter was the EM38, manufactured by Geonics Limited*. The meter is portable and requires only one person to operate. Principles of operation have been described by McNeill (1986). The observation depth of an EM meter is dependent upon intercoil spacing, transmission frequency, and coil orientation relative to the ground surface. The EM38 meter has a fixed intercoil spacing of about 1.0 m. It operates at a frequency of 13.2 kHz. The EM38 meter has effective observation depths of about 0.75 and 1.5 m in the horizontal and vertical dipole orientations, respectively (McNeill, 1986). Values of apparent conductivity are expressed in milliSiemens per meter (mS/m).

The radar unit used in this study was the Subsurface Interface Radar (SIR) System-2, manufactured by Geophysical Survey Systems, Inc. (GSSI)*. The use and operation of GPR have been discussed by Morey (1974), Doolittle (1987), and Daniels and others (1988). The SIR System-2 consists of a digital control unit (DC-2) with keypad, VGA video screen, and connector panel. Radar profiles were plotted on a model GS-608P thermal plotter/printer. The system was powered by a 12-VDC battery. The model 3110 (120 MHz) and 3105 (300 MHz) antennas were used in this investigation.

The radar profile included in this report was processed through RADAN software. Processing was limited to signal stacking, horizontal scaling, compression, customizing color transform and color tables, and annotations.

To help summarize the results of this study, the SURFER for Windows program, developed by Golden Software, Inc.,* was used to develop two- and three-dimensional simulations. Grids were created using kriging methods with an octant search. All grids were smoothed using cubic spline interpolation.

Field Methods

A grid had been established in the extreme southwestern portion of the research watershed. The grid covered about 9.4 hectares. The grid interval was about 20 m. Grid lines and intersections were established with a compass and hip chain. At each of the 166 grid intersections, survey flags were inserted in the ground. The coordinates of each grid intersection were tied into a base map of the research watershed. The surface elevation of each grid intersection was inferred from the base map. The location of the 20 meter grid is considered imprecise and the placement of major grid intersections, the detailed grid site, and traverse lines on the enclosed computer simulations will be improved (at a later date) using GPS.

* Trade names are used to provide specific information. Their mention does not constitute endorsement by USDA-NRCS.

At each of the 166 grid intersections of the 20-m grid, measurements were obtained with an EM38 meter in both the horizontal and vertical dipole orientations.

Within the 20-m grid, a smaller grid had been established immediately upslope from a research trench. The interval of this grid was 2 m. A GPR survey was conducted on an irregularly shaped, 30 by 20 m portion of this grid. The GPR survey was conducted by pulling the 300 MHz antenna along parallel grid lines in an upslope or downslope direction.

Additional radar profiles were collected along three traverse lines in the study site (see Figure 2), and along several trails within the research watershed.

Electromagnetic Induction

Background:

Electromagnetic induction is a non-invasive geophysical technique which uses electromagnetic energy to measure the apparent conductivity of earthen materials. Apparent conductivity is a weighted average measurement for a column of earthen materials to a specified observational depth (Greenhouse and Slaine, 1983). Variations in apparent conductivity are produced by changes in the electrical conductivity of soils and other earthen materials. The electrical conductivity of soils is influenced by the (i) volumetric water content, (ii) type and concentration of ions in solution, (iii) temperature and phase of the soil water, and (iv) amount and type of clay in the soil matrix (McNeill, 1980). The apparent conductivity of soils increases with increases in the exchange capacity, water content, and clay content (Kachanoski et al., 1988; Rhoades et al., 1976).

Soil scientists have used EM techniques principally to identify, map, and monitor soil salinity (Cook and Walker, 1992; Corwin and Rhoades, 1982, 1984, and 1990; Rhoades and Corwin, 1981; Rhoades et al., 1989; Slavich and Petterson, 1990; Williams and Baker, 1982; and Wollenhaupt et al., 1986). Recently, the use of this technology has been expanded to include the assessment and mapping of sodium-affected soils (Ammons et al., 1989; Nettleton et al., 1994), depths to claypans (Sudduth and Kitchen, 1993; Stroh et al., 1993; and Doolittle et al., 1994), and edaphic properties important to forest site productivity (McBride et al., 1990).

Though seldom diagnostic in themselves, lateral and vertical variations in apparent conductivity have been used to infer changes in soils and soil properties. Electromagnetic induction is not suitable for use in all soil investigations. Generally, the use of EM techniques has been most successful in areas where subsurface properties are reasonably homogeneous, the effects of one property (e.g. clay, water, or salt content) dominates over the other properties, and variations in EM response can be related to changes in the dominant property (Cook et al., 1989).

Discussion:

Figures 3 and 4 are two-dimensional plots of apparent conductivity measurements simulated from data collected with the EM38 meter in the horizontal and vertical dipole orientations, respectively. Within the study site, values of apparent conductivity were exceedingly low and relatively invariable. Apparent conductivity averaged 1.95 and 0.03 mS/m

in the horizontal and vertical dipole orientations, respectively. Within the study site, values of apparent conductivity obtained with the EM38 meter ranged from -0.2 to 8.5 mS/m and from -4.1 to 2.0 mS/m in the horizontal and vertical dipole orientations, respectively.

Electromagnetic induction measurements obtained within the study site were considered exceptionally low for medium- and fine-textured (18 to > 35 percent clay) soil materials. However, these measurements are considered representative of highly weathered soils having low base saturation, high proportion of low activity clays (kaolinite, gibbsite), and with relatively shallow depths to highly resistive materials (granite bedrock or saprolite). In general, electromagnetic responses decreased with increasing soil depth. This relationship reflects the presence of slightly more conductive soil materials (i.e. higher clays and/or water contents) overlying more electrically resistive granite bedrock.

The isolines appearing in figures 3 and 4 are believed to reflect changes in soils, soil properties, and/or soil depth, and the influence of the underlying saprolite and granite bedrock. In each plot, the isoline interval is 1 mS/m. Comparing figures 2 and 3, iso-conductivity lines are more closely spaced along the drainageway, on concave footslopes, and on convex shoulder and summit positions. In addition, electromagnetic gradients appear to be more variable on south- and east-facing slopes than on north and west-facing slopes. Iso-conductivity lines are further apart and properties are assumed to be more homogeneous in areas of rock outcrops in the northwestern and southern portions of the survey site. In general, with the EM38 meter, areas of rock outcrop had values of less than 1 mS/m in both orientations.

In Figure 3, spatial patterns conform with major soil delineations mapped within the study site (Mount et al., in preparation). Electromagnetic measurements were generally lower in areas of Ashlar and Wake soils, and rock outcrops. Typically, these areas are shallower to bedrock than are other areas of the study site. Higher EM responses were recorded in areas of Madison, Rion, and Toccoa soils. These soils are deeper to bedrock and occur on summits, convex shoulder slopes, and concave footslopes.

The low and relatively invariable response of the EM38 meter in the vertical dipole orientation (Figure 4) was assumed to reflect the increased influence of the underlying, more electrically resistive saprolite and granite bedrock. McNeill (1980) reported a resistivity range of 3×10^2 to 10^6 ohm-meters for granite. This range corresponds to values of apparent conductivity ranging from 0.0003 to 3.0 mS/m. At these exceptionally low values of apparent conductivity, small errors in calibration are greatly magnified. As a consequence, some of the spatial patterns evident in both plots of apparent conductivity values (figure 3 and 4), but principally in Figure 4, are assumed to be the result of calibration and observation errors rather than changes in apparent conductivity.

In the vertical dipole orientation, one half of the observations, had EM responses ranging from -0.40 to 0.50 mS/m. As a result of this exceedingly low and narrow range in EM measurement, data collected in the vertical dipole orientation provided little meaningful information concerning the study site. However, in Figure 4, one noticeable pattern is evident. Apparent conductivity measurements were exceedingly low (-1 to -3 mS/m) in the extreme southwestern portion of the study site. This

area of low apparent conductivity values corresponded with the only delineation of Madison soils within the study site. Surprisingly, in this area of Madison soils, EM responses were lowest in the vertical dipole orientation (Figure 4) and among the highest in the horizontal dipole orientation (Figure 3). Other than corresponding with a particular soil type, the significance of this relationship remains obscured.

No conspicuous spatial patterns were evident in the plot of the measurements collected with the EM38 meter in the vertical dipole orientation. This was assumed to reflect the highly electrically resistive and relatively invariable properties of the underlying Panola Granite, and possibly the effects of calibration errors and the geometry of current flow in this orientation.

Figure 5 is a three-dimensional representation showing the distribution of EM38 measurements collected in the horizontal dipole orientation with surface topography across the study site. Pattern are assumed to reflect changes in soils, soil properties, and/or saprolite depth and thickness with hillslope positions. These spatial patterns suggest that these relatively shallow measurements are more variable on south-facing slopes and along the head slope of the drainageway.

In Figure 5, a linear pattern of higher EM responses extends in a north-northeast to south-southwest direction along the drainageway. This linear pattern extends from the head slope of the drainageway across the site. In a study conducted by Olayinka (1990) in Nigeria, areas of high electrical conductivity were identified and associated with zones of deep weathering and/or fracture zones in crystalline bedrock. The linear pattern recognized in Figure 5, though reflecting near-surface conditions, could reflect not only changes in soil types, but a zone of deeper weathering and/or fracture traces in the underlying bedrock. Hopefully, this possible relationship will be confirmed by the knocking-pole penetrometer measurements conducted by Al Zumbuhl

Within the study site, the response of the EM38 meter in the shallow (0 to 75 cm) horizontal dipole orientation was associated with difference in soil types and depths. No apparent relationship could be inferred from the response of the EM38 meter in the deeper sensing (0 to 150 cm), vertical dipole orientation. As EM measurements integrate the bulk physical and chemical properties for a defined observational depth into a single value, responses can be associated with changes in soils and soil map units (Hoekstra et al., 1992; Jaynes et al., 1993). For each soil, the inherent variability in physical and chemical properties, as well as temporal variations in soil water and temperature, will establish a characteristic range of observable apparent conductivity values. This range can be influenced by differences in use or management practices (Sudduth and Kitchen, 1993).

Ground-penetrating radar:

Background:

Ground-penetrating radar is an impulse radar system designed for shallow, subsurface investigations. This system operates by transmitting short pulses of electromagnetic energy into the ground from an antenna. Each pulse consists of a spectrum of frequencies distributed around the center frequency of the transmitting antenna. Whenever a pulse contacts an

interface separating layers of differing electromagnetic properties, a portion of the energy is reflected back to the receiving antenna. The receiving unit amplifies and samples the reflected energy and converts it into a similarly shaped waveform in a lower frequency range. The processed reflected waveforms are displayed on a VGA video screen, printed on a thermal recorder, or are stored on an internal disk drive for future playback and/or post-processing.

Soil scientist have used GPR to estimate depth to argillic (Asmussen et al., 1986; Truman et al. 1988a and 1988b; Collins and Doolittle, 1987; Hubbard et al., 1990), and spodic horizons (Doolittle, 1987; Collins and Doolittle, 1987), to infer soil color or organic carbon content of spodic horizons (Doolittle, 1982; Collins and Doolittle, 1987), to assess the concentration of roots (Truman et al., 1988b) or lamellae of finer textured soil materials (Farrish et al., 1990; Mokma et al., 1990), to illustrate soil-bedrock relations on glacial-scoured uplands (Doolittle et al., 1988; Collins et al., 1989) and on karst (Collins et al., 1990; Puckett et al., 1990) and the subsurface topography of cranberry bogs (Doolittle et al., 1990a), and to determine thickness of surface (Doolittle, 1987) and active layers (Doolittle et al. 1990b). In addition, GPR has been used to study changes in soil properties which affect forest productivity (Farrish et al., 1990) and stress in citrus trees (Shih et al. 1985).

Interpretations:

A. The radar profile -

Reflected radar waveforms were plotted on a raster-scan, thermal plotter/printer. Through a thermo-chemical reaction, radar images are developed as thermal sensitive paper is moved under a fixed thermal printhead. The intensity of these images are dependent upon the amplitude of the reflected signals.

Figure 6 is an example of a radar profile. The horizontal scale represents units of distance traveled along an antenna traverse. This scale is dependent upon the speed of antenna advance along a traverse line and the rate of paper advance through the thermal plotter. The vertical scale is a time or depth scale which is based on the velocity of signal propagation.

The four basic components of a radar profile have been identified in Figure 6. These components are the start of scan pulse (A), inherent antenna noise (B), surface image (C), and subsurface interface images (D). Each of these components, with the exception of the start of scan pulse, is generally displayed as a group of dark bands. The number of bands can be limited by high rates of signal attenuation or superimposed signals. These bands limit the ability of GPR to discriminate closely spaced interfaces. The dark bands occur at both positive and negative signal amplitudes. The narrow white band(s) separating the darker bands represent the neutral or zero crossing between positive and negative signal amplitudes.

The start of scan image (see A in Figure 6) results from direct feed-through of transmitted pulses into the receiver section of the antenna. Though a source of unwanted clutter, the start of scan pulse is often used as a time reference line.

Reflections unique to each of the system's antennas are the first series of multiple bands on radar profiles. Generally the width of these bands increases with decreasing antenna frequency or signal filtration. These reflection (see B in Figure 6) are a source of unwanted noise on radar profiles.

The surface image (see C in Figure 6) represents the ground surface. Below the image of the surface reflection are images from subsurface interfaces (see D in Figure 6). Interfaces can be categorized as being either plane or point reflectors. Most soil horizons and geologic strata appear as a series of continuous, parallel bands similar to those appearing in Figure 6. Features that produce these reflections are referred to as "plane reflectors." Small objects such as rocks, roots, or buried cultural features can produce a hyperbolic pattern similar to the feature appearing (weakly expressed) to the right of E in Figure 6. Features that produce these reflections are referred to as "point reflectors."

B. Calibration -

Generally, for most soil investigations, auger or coring data as well as exposures and observation pits are used to verify interpretations and confirm the depths to known reflectors. These data are used to determine the depth scale(s). However, in this study, few observations and no deep corings were made to confirm interpretations or observation depths. In this study, the large physical size of the watershed, the diversity of soils and soil properties, and the lack of adequate ground truth verifications limited the number of interpretations which could be made with confidence from the radar profiles.

The GPR is a time scaled system. This system measures the time that it takes electromagnetic energy to travel from the antenna to an interface (e.g. soil horizon, stratigraphic layer, bedrock surface) and back. In order to convert the travel time into a depth scale, either the velocity of pulse propagation or the depth to a reflector must be known. The relationship among depth (d), two-way, pulse travel time (t), and velocity of propagation (v) are described in the following equation (Morey, 1994):

$$v = 2d/t$$

The velocity of propagation is principally affected by the dielectric constant (e) of the profiled material(s) according to the equation:

$$e = (c/v)^2$$

where c is the velocity of propagation in a vacuum (0.3 m/s). The amount and physical state (temperature dependent) of water has the greatest effect on the dielectric constant of a material. Tabled values are available that approximate the dielectric constant of some materials (Morey, 1974; Petroy, 1994). However, as discussed by Daniels and others (1988), these values are simply approximations.

Calibration trials were conducted near the trench and grid site, and in an area of Ashlar soils. In these trials, scanning times of 60, 100, and 150 ns were used. The purposes of these trials were to determine the dielectric constant and velocity of propagation of electromagnetic energy

through the surface soil layers, establish a crude depth scale, and optimize control and recording settings.

During calibration trials, multiple traverses were conducted with the 120 MHz antenna. A scanning rate of 32 scans/sec was used in these trials and in all subsequent field work. Considerations of desired versus achievable depths of observation and the resolution of subsurface features influenced the selection of scanning times. Both the 300 and 120 MHz antennas provided acceptable depths of observation.

Based on a known depth (48 cm) to a buried reflectors, the velocity of propagation through the surface soil layers and a depth scale for radar profiles were estimated. Based on the round-trip travel time to this reflector, the velocity of propagation was estimated to be 0.067 m/ns. The dielectric constant was estimated to be 20.5. The estimated dielectric constant was higher and the velocity of propagation was lower than anticipated. The dielectric constant is within the range for clayey (5-40) and silty (5-30) soil materials, but slightly higher than tabled values for wet loamy (19) soil materials (Petroy, 1994). However, considering that the fringes of a hurricane past over the watershed on June 5 and the surface layers were moist, these values were considered close approximations. However, it is necessary to state that errors are often introduced into the interpretation of radar records from similar, superficial examinations of soils or from values for these parameters deduced from the literature (Tillard and Dubois, 1995).

As the reflector was buried at a depth of less than 50 cm, the estimated velocity of propagation and dielectric constant were appropriate for only the surface layers in an area of excessively drained, medium-textured soil. As radar traverses crossed several soils and numerous subsurface layers of variable compositions, no single value is appropriate for either the dielectric constant or velocity of propagation. As a large proportion of the traverses were conducted in areas having medium to fine-textured soil materials and shallow to very deep depths to saprolite or bedrock, the estimated dielectric constant and velocity of propagation (20.5 and 0.067 m/ns, respectively) should be viewed as providing merely an approximate estimate of the depth of observation. Based on these values, scanning times of 60, 100, 150, and 200 ns would provide maximum observation depths of about 2.0, 3.4, 5.0, and 6.7 m, respectively.

C. Performance -

Ground-penetrating radars do not perform equally well in all soils. The maximum observation depth of GPR is, to a large degree, determined by the conductivity of the soil and geologic materials. Materials having high electrical conductivities rapidly dissipate the radar's energy and restrict the depth of observation. The principal factors influencing the conductivity of soils and geologic materials to electromagnetic radiation are: (i) degree of water saturation, (ii) the amount and type of clay, and (iii) the amount and type of salts in solution.

Electromagnetic conductivity is essentially an electrolytic process that takes place through moisture filled pores. As water-filled porosity is increased, the velocity of signal propagation is reduced, the rate of signal attenuation is increased, and the observation depth of the radar is reduced. For the purpose of this investigation, it was assumed that water contents were relatively uniform in the surface layers, increased with soil depth and clay content, and decreased with rock content. The

water-filled porosity was assumed to be greater in areas underlain by saprolite or fractured bedrock than in areas underlain by coherent bedrock.

Electrical conductivity is directly related to the concentration of dissolved salts in the soil solution. Ions adsorbed to clay particles can undergo exchange reactions with ions in the solution and thereby contribute to the electrical conductivity of soils and geologic materials. The concentration of ions in solution is dependent upon the clay minerals present, the relative proportion of ions on exchange sites, the degree of water filled porosity, the pH of the solution, and the nature of the ions in solution. For the purpose of this investigation, it was assumed that the soils have formed from similar geologic materials (granite), have low and similar base saturations, and were slightly to extremely acid in reaction. Within the Panola Mountain Research Watershed, the concentration of dissolved salts were assumed to be low and not a limiting factor to GPR.

Soil texture (clay content) and mineralogy strongly influence the performance of GPR. The maximum observation depth of GPR increases as the clay content decreases. Generally, maximum observation depths are about 5 to 25 meters in coarse textured soils, 2 to 5 meters in moderately-coarse textured soils, 1 to 2 meters in moderately-fine textured soils, and less than 0.5 to 1.5 meters in fine textured soils. As discussed earlier, observation depths increase as the proportion of low activity clays increases. For the purpose of this investigation, it was initially assumed that observation depths of 0.5 to 2 meters could be attained in the highly weathered soils of the watershed. However, prior to this investigation, negligible work had been conducted in Piedmont soils by this investigator. As a consequence, a great deal of uncertainty surrounded the depth of observation and the appropriateness of using GPR techniques within the watershed.

The amount of energy reflected back to an antenna from a subsurface interface is a function of the dielectric gradient existing between the adjoining materials. The greater or more abrupt the difference in dielectric properties, the greater the amount of energy reflected back to the antenna, and the more intense will be the amplitude of the image recorded on the radar profile. The typical sequence of layered materials within the watershed was soil-saprolite-bedrock. Saprolite consists of soft, friable, weathered bedrock that retains some of the structure of the parent rock. The term, "saprolite," has been applied to unconsolidated residual materials underlying soils and grading to hard bedrock below (Soil Survey Staff, 1993). Because saprolite represents a gradational or transitional material, the capacity of GPR to detect and define the soil/saprolite and the saprolite/bedrock interface was unknown.

The radar profiles obtained within the watershed contained reflections from numerous, often segmented soil horizons, and stratigraphic and lithologic layers. Typically, the layers varied laterally in expression. On some radar profiles, reflections from these layers were poorly expressed or partially masked by adjacent strata. The radar detects but does not identify subsurface interfaces. In areas where subsurface layers are numerous or segmented, a large number of auger or coring observations are required to satisfactorily interpret the radar profiles. During this brief investigation, it was not possible to obtain an adequate number of observations.

Discussion:

General:

This study was the first opportunity that I had to operate the SIR System-2 unit in the carrying harness. Difficulties were initially encountered conducting the radar survey in a steep, forested terrain, establishing the correct settings on the digital control unit (DC-2), and recharging the portable batteries. These obstacles were overcome with experience and some improvisation. The inoperative battery recharger was later repaired.

The SIR System-2 unit was found to be a robust, highly portable unit suitable for rapidly traversing most forested areas. Pulling the antenna (especially the 120 MHz) required greater effort than carrying the control unit with portable battery. As restrictions were imposed on the amount of disturbance permitted, survey lines were often adjusted to avoid trees, fallen tree limbs, vines and bushes.

Throughout most of the watershed, depths of observation were less restricted than anticipated and many subsurface features were evident on the radar profiles. The depth of observation appears to be related to the mica content of Piedmont soil. Cecil and Madison soils are members of the clayey, kaolinitic, thermic Typic Kanhapludults family. Both soils are well drained and very deep to bedrock. Typically, with the 120 MHz antenna, the maximum depth of observation was greater than 6.0 m (estimated from scanning times of 150 to 200 ns) in areas of Cecil soils, but less than 1 meter in areas of Madison soils. This disparity in observation depths for similar soils was attributed principally to differences in the amount of mica flakes in each soil. The amount of mica flakes in Madison soils is higher than in Cecil soils. It was assumed that the mica flakes act as conductors to electromagnetic energy. These micaceous conductors dissipate the transmitted and reflected energy of the radar and thereby limit the depth of observation. Because of the lack of "ground-truth" observations and samples, this inference could not be confirmed. Concerns were also expressed as to the influence of saprolite on the observation depth of GPR. Hopefully, further investigations with GPR will assess the influence of mica flakes and saprolite on the observation depth of GPR.

Figure 7 is a representative radar profile from the 2-meter grid site. The location of the 2-m grid within the study site is shown in Figure 2. This profile has been processed through RADAN software. The radar profile has been stacked and normalized. Signal stacking can reduce incoherent background noise while enhancing the image of bedrock surfaces. Often, because of noise suppression, stacked traces have considerably more discernible features especially at greater depths. Normalization corrects the horizontal scale for variations in the speed of antenna advance along a grid line. The general location and trend of some subsurface interfaces have been approximated with dark lines. These lines have been drawn to emphasize the depth, extent, and characteristics of the inferred saprolite and bedrock surfaces.

The horizontal scale represents units of distance traveled along a grid line. The numbers appearing at the top of the radar profile represent distances in meters. The segmented, vertical lines are grid intersections and occur at 2 m intervals. The vertical scale is a time or depth scale, which is based on the estimated velocity of signal propagation (0.067 m/ns) from the calibration site. In this figure, the

depth of observation is about 2 meters (see scale along left-hand margin).

In Figure 7, three subsurface features have been identified: the (1) saprolite and (2) bedrock surfaces and a (3) metallic point reflector (reverberated signals enclosed in a rectangular box). The point reflector was a metallic survey flag which was run over by the antenna (see Figure 7, below the 30 m mark). The subsurface reflector believed to be the bedrock surface consisted of three strong, nearly continuous, subsurface reflections. The image of the bedrock surface varies laterally in expression. This variability was presumed to be related to differences in the degree of weathering, thickness, and/or occurrence of saprolite, and the abruptness of the electromagnetic gradient between the saprolite and bedrock. In some areas, the image of the bedrock surface was indistinct from the saprolite or was masked by the presence of closely-spaced, overlying features (i.e. rock fragments, soil/saprolite interface).

Attempts to consistently identify the soil/saprolite interface on radar profiles were problematic. Without processing through the RADAN software program, this interface was difficult to perceive with any degree of reliability. Even with processing, the upper boundary of the saprolite produces weak reflections and indistinct images on most radar profiles. Because of the weak reflection from the soil/saprolite interface, it was assumed that the electromagnetic gradient was gradual and/or dielectric properties were weakly contrasting between these two materials.

To confirm the precision of GPR for determining the depths to saprolite or bedrock, scaled radar depths were compared with depths observed in auger observations at grid intersection along a grid line (16 observations). Along the grid line, the average observed depth to saprolite was 60.5 cm with a range of 25 to 128 cm. The average difference between the observed and interpreted depth to saprolite was 11.1 cm. Eighty-seven percent of the scaled radar imagery was within 0 to 18 cm of the actual depth to saprolite. However, the correlation between observed and scaled depths was low ($r^2 = 0.38$). The lack of a stronger relationship between observed and scaled depths to saprolite was attributed to spatial discrepancies between the points of auger and radar observations, observation errors, and irregularities in the saprolite surface. At best, the radar passed within 50 cm of each observation sites. Tree limbs and brush often necessitated the antenna being pulled at a greater distance from the grid line. In addition, auger observations are often plagued with uncertainties as to whether probings were halted by the bedrock or saprolite surface or by a large rock fragment.

Table 2

Depth to Bedrock/Saprolite
2-m Grid Site

Depth (cm)	Frequency (%)
0 to 50	25
50 to 100	71
100 to 150	04
>150	00

The radar survey, was completed in less than one 1.0 hr. The survey consisted of about 294 meters of continuous radar records. Based on radar interpretations at 158 observation points, the depth to bedrock/or saprolite ranged from about 26 to 123 cm. Within the study site, the average depth to bedrock/saprolite was about 63.78 cm. One-half of the observations had deposits between 49 and 75 cm. Table 2 summarizes the distribution of soil depths.

Figure 8 and 9 are two-dimensional plots of the depth to bedrock or saprolite within the 2-m grid site. In Figure 9, to help emphasize the spatial distribution of soil depths, color shading and filled contour lines have been used. Other than showing trends in soil depths, no significance should be attached to the colors themselves. A bedrock outcrop occurred in the area which was not surveyed in the upper left-hand corner of the plots

In figures 8 and 9, an area of moderately deep (50 to 100 cm) and deep (100 to 150 cm) soils extends across the lower-central portion of the grid site. The orientation of this zone of deeper soils is essentially parallel with the contour. Areas of shallow soils occur in the upper and lower right-hand portions of the site.

Results:

1. Within the study site, soils and bedrock were characterized as having exceedingly low apparent conductivities. Soils are highly weathered and have low base saturations and cation exchange capacities. Variations in the EM measurements obtained in the horizontal dipole orientation (0 to 75 cm) appeared to be associated with differences in soil type and depths. The underlying Panola Granite is extremely electrically resistive and produced apparent conductivity values so low that they were essentially immeasurable with the EM38 meter in the vertical dipole orientation (0 to 150 cm).

2. Ground-penetrating radar techniques can be used effectively for pedological investigations in many portions of the watershed. In general, Piedmont soils were less restrictive to GPR than expected. **These soil are characterized as being highly weathered, having low base saturations and dominated by low activity clays.** Even in some clayey soils, such as Cecil, depths of observation exceeded expectations. In some clayey soils, such as Madison, depths were more restricted. Though more research is necessary, depths of GPR observation appear to be associated with the mica content of soils.

The soil/saprolite interface was difficult to identify on radar profiles. Even with processing, the upper boundary of the saprolite produced weak reflections and indistinct images on most radar profiles. Additional studies are needed to optimize settings on the control unit and to improve interpretations. Interpretations can only be improved with repeated field studies supported by sufficient "ground truth" verifications.

The correlation between the observed (soil auger) and the interpreted (GPR) depths to bedrock was lower ($r^2 = 0.38$) than anticipated. Several

probable causes for this low correlation have been identified in this report. Additional studies are again recommended.

3. I regret that time did not permit a more comprehensive evaluation of the potential uses and limitations of these geophysical tools within the catchment. We have left more questions unanswered than answered. Further research with these tools is encouraged.

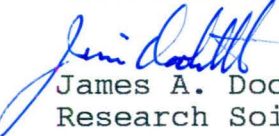
4. All radar profiles have been returned to Al Zumbuhl for use in his research. In addition all radar profiles have been stored on tapes and will be maintained in my office. The example provided in this report is highly interpretative and for general guidance only. Persons more familiar with saprolite and Piedmont soils should analyze and help interpret the radar profiles. Ground-truth corings are needed and are essential to confirm interpretations.

5. Upon request and with advanced notice, select portions of the radar profiles can be processed and made available.

6. A rather extensive but not exhaustive list of references have been included in this report. These articles may be of assistance to Al Zumbuhl in his research.

7. I am very pleased to have had the opportunity to work with the research assistants from SUNY CESF. I hope that the co-operative spirit which pervaded this study will be extended into other field investigations.

With kind regards


James A. Doolittle
Research Soil Scientist

cc:

James Culver, Assistant Director, NSSC, NRCS, Lincoln, NE
Steve Holzhey, Assistant Director, NSSC, NRCS, Lincoln, NE
Al Zumbuhl, One Forestry Drive, State University of New York, College of
Environmental Science and Forestry, Syracuse, New York 13210-2778

References

- Asmussen, L. E., H. F. Perkins, and H. D. Allison. 1986. Subsurface Descriptions by ground-penetrating radar for watershed delineation. The Georgia Agricultural Experiment Stations Research Bulletin No. 340. Univ. of Georgia, Athens. pp. 15.
- Ammons, J. T., M. E. Timpson, and D. L. Newton. 1989. Application of aboveground electromagnetic conductivity meter to separate Natraqualfs and Ochraqualfs in Gibson County, Tennessee. Soil Survey Horizons 30(3):66-70.
- Collins, M. E., and J. A. Doolittle. 1987. Using ground-penetrating radar to study soil microvariability. Soil Sci Soc. Am. J. 51:491-493.
- Collins, M. E., J. A. Doolittle, and R. V. Rourke. 1989. Mapping depth to bedrock on a glaciated landscape with ground-penetrating radar. Soil Science Society of America J. 53:1806-1812.
- Collins, M. E., W. E. Puckett, G. W. Schellentrager, and N. A. Yust. 1990. Using GPR for micro-analyses of soils and karst features on the Chiefland Limestone Plain in Florida. Geoderma 47:159-170.
- Cook, P. G., M. W. Hughes, G. R. Walker, and G. B. Allison. 1989. The calibration of frequency-domain electromagnetic induction meters and their possible use in recharge studies. Journal of Hydrology 107:251-265.
- Cook, P. G. and G. R. Walker. 1992. Depth profiles of electrical conductivity from linear combinations of electromagnetic induction measurements. Soil Sci. Soc. Am. J. 56:1015-1022.
- Corwin, D. L., and J. D. Rhoades. 1982. An improved technique for determining soil electrical conductivity-depth relations from above-ground electromagnetic measurements. Soil Sci. Soc. Am. J. 46:517-520.
- Corwin, D. L., and J. D. Rhoades. 1984. Measurements of inverted electrical conductivity profiles using electromagnetic induction. Soil Sci. Soc. Am. J. 48:288-291.
- Corwin, D. L., and J. D. Rhoades. 1990. Establishing soil electrical conductivity - depth relations from electromagnetic induction measurements. Communications in Soil Sci. Plant Anal. 21(11&12):861-901.
- Daniels, D. J., D. J. Gunton, and H. F. Scott. 1988. Introduction to subsurface radar. IEE Proceedings 135F(4):278-320.
- Doolittle, J. A. 1982. Characterizing soil map units with the ground-penetrating radar. Soil Survey Horizons 22(4):3-10.
- Doolittle, J. A. 1987. Using ground-penetrating radar to increase the quality and efficiency of soil surveys. IN Soil Survey Techniques, Soil Science Society of America Special Publ. No 20. pp. 11-32.
- Doolittle, J. , P. Fletcher, and J. Turenne. 1990a. Estimating the thickness and volume of organic materials in cranberry bogs. Soil Survey Horizons 31(3)73-78.
- Doolittle, J. A., M. A. Hardisky, and M. F. Gross. 1990b. A ground-penetrating radar study of active layer thicknesses in areas of moist

- sedge and wet sedge tundra near Bethel, Alaska, U.S.A. *Arctic and Alpine Research* 22(2):175-182.
- Doolittle, J. A., R. A. Rebertus, G. B. Jordan, E. I. Swenson, and W. H. Taylor. 1988. Improving soil-landscape models by systematic sampling with ground-penetrating radar. *Soil Survey Horizons*. 29(2):46-54.
- Doolittle, J. A., K. A. Sudduth, N. R. Kitchen, and S. J. Indorante. 1994. Estimating depth to claypans using electromagnetic inductive methods. *J. Soil and Water Conservation* 49(6):552-555.
- Greenhouse, J. P., and D. D. Slaine. 1983. The use of reconnaissance electromagnetic methods to map contaminant migration. *Ground Water Monitoring Review* 3(2):47-59.
- Farrish, K. W., J. A. Doolittle, and E. E. Gamble., 1990. Loamy substrata and forest productivity of sandy glacial drift soils in Michigan. *Canadian Journal of Soil Science* 70:181-187.
- Hubbard, R. K., L. E. Asmussen, and H. F. Perkins. 1990. Use of ground-penetrating radar on upland Coastal Plain soils. *Journal of Soil and Water Conservation*. p. 399-404.
- Huntington, T. G., R. P. Hooper, N. E. Peters, T. D. Bullen, and C. Kendall. 1993. Water, energy, and biogeochemical budgets investigation at Panola Mountain Research Watershed, Stockbridge, Georgia -- A Research plan. U. S. Geological Survey Open File Report 93-55. pp. 39.
- Hoekstra, P., R. Lahti. J. Hild, R. Bates, and D. Phillips. 1992. Case histories of shallow time domain electromagnetics in environmental site assessments. *Ground Water Monitoring Review*. 12(4):110-117.
- Jaynes, D. B., T. S. Colvin, J. Ambuel. 1993. Soil Type and crop yield determination from ground conductivity surveys. 1993 International Meeting of American Society of Agricultural Engineers. Paper No. 933552. ASAE, St. Joseph, MI. pp. 6.
- Kachanoski, R. G., E. G. Gregorich, and I. J. Van Wesenbeeck. 1988. Estimating spatial variations of soil water content using noncontacting electromagnetic inductive methods. *Can. J. Soil Sci.* 68:715-722.
- McBride, R. A., A. M. Gordon, and S. C. Shrive. 1990. Estimating forest soil quality from terrain measurements of apparent electrical conductivity. *Soil Sci. Soc. Am. J.*, 54:290-293.
- McNeill, J. D. 1980. Electrical Conductivity of soils and rocks. Technical Note TN-5. Geonics Ltd., Mississauga, Ontario. pp. 22.
- McNeill, J. D. 1986. Geonics EM38 ground conductivity meter operating instructions and survey interpretation techniques. Technical Note TN-21. Geonics Ltd., Mississauga, Ontario. pp. 16.
- Mokma, D. L., R. J. Schaetzl, E. P. Johnson, and J. A. Doolittle. 1990. Assessing Bt horizon character in sandy soils using ground-penetrating radar: Implications for soil surveys. *Soil Survey Horizons*. 30(2):1-8.
- Morey, R. M. 1974. Continuous subsurface profiling by impulse radar. pp. 212-232. In: Proceedings, ASCE Engineering Foundation Conference on

Subsurface Exploration for Underground Excavations and Heavy Construction, held at Henniker, New Hampshire. Aug. 11-16, 1974.

Mount, H., T. Gerald, and L. West. (in preparation). Soil Survey of Panola Mountain Research Watershed. USDA Natural Resources Conservation Service.

Nettleton, W. D., L. Bushue, J. A. Doolittle, T. J. Endres, and S. J. Indorante. 1994. Sodium-affected soil identification in south-central Illinois by electromagnetic induction. *Soil Sci. Soc. Am. J.* 58:1190-1193.

Olayinka, A. I. 1990. Electromagnetic profiling for groundwater in Precambrian basement complex areas of Nigeria. *Nordic Hydrology* 21:205-216.

Petroy, D. E. 1994. Assessment of ground-penetrating radar applicability to specific site investigations: Simple methods for pre-survey estimation of likely dielectric constants, target resolution and reflection strengths. SAGEEP '94'. Symposium on the Application of Geophysics to Engineering and Environmental Problems. 27 to 31 March 1994. Boston, Massachusetts. pp. 21.

Puckett, W. E., M. E. Collins, and G. W. Schellentrager. 1990. Design of soil map units on a karst area in West Central Florida. *Soil Science Society of America J.* 54:1068-1073.

Rhoades, J. D. and D. L. Corwin. 1981. Determining soil electrical conductivity-depth relations using an inductive electromagnetic soil conductivity meter. *Soil Sci. Soc. Am. J.* 45:255-260.

Rhoades, J. D., N. A. Manteghi, P. J. Shouse, and W. J. Alves. 1989. Soil Electrical conductivity and soil salinity: new formulation and calibrations. *Soil Sci. Soc. Am. J.* 53:433-439.

Rhoades, J. D., P. A. Raats, and R. J. Prather. 1976. Effects of liquid-phase electrical conductivity, water content, and surface conductivity on bulk soil electrical conductivity. *Soil Sci. Soc. Am. J.* 40:651-655.

Slavich, P. G. and G. H. Petterson. 1990. Estimating average rootzone salinity from electromagnetic induction (EM-38) measurements. *Australian J. Soil Res.* 28:453-463.

Shih, S. F., D. L. Myhre, G. W. Schellentrager, V. W. Carlisle, and J. A. Doolittle. 1985. Using radar to assess the soil characteristics related to citrus stress. *Soil and Crop Science of Florida, Proc.* 45:54-59.

Soil Survey Staff. 1993. National Soil Survey Handbook. U. S. Department of Agriculture, Soil Conservation Service. U. S. Government Printing Office, Washington, D. C.

Stroh, J., S. R. Archer, L. P. Wilding, and J. Doolittle. 1993. Assessing the influence of subsoil heterogeneity on vegetation patterns in the Rio Grande Plains of south Texas using electromagnetic induction and geographical information system. College Station, Texas. *The Station* (Mar 93):39-42.

Sudduth, K. A. and N. R. Kitchen, 1993. Electromagnetic induction sensing of claypan depth. Paper No. 93-1550. Presented at the December 1993, Winter Meetings of the American Society of Agricultural Engineers. St. Joseph, Michigan. pp. 18.

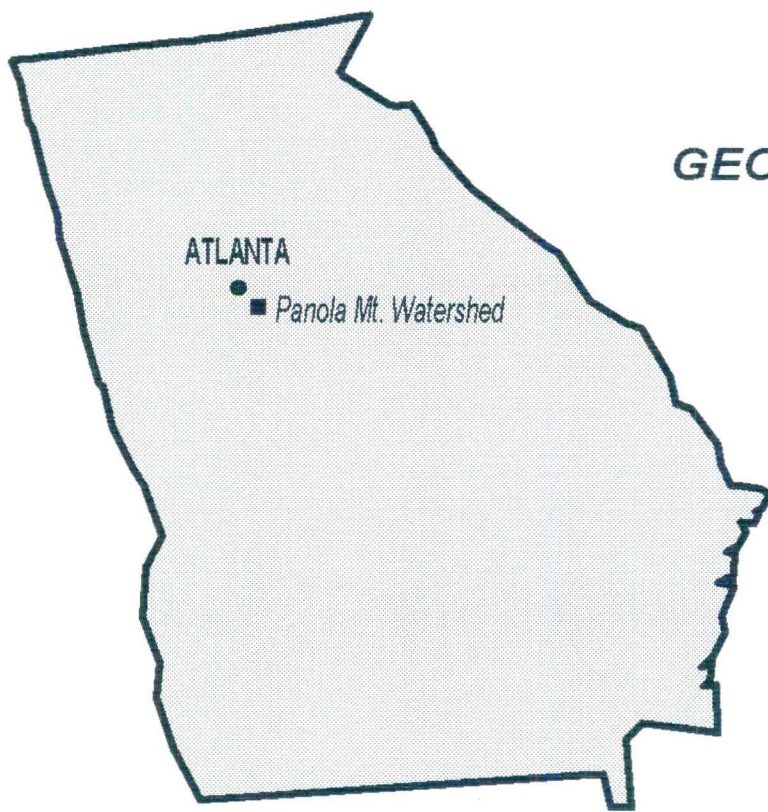
Tillard, S. and J. C. Dubois. 1995. Analysis of GPR data: wave propagation velocity determination. Journal of Applied Geophysics 33: 77-91.

Truman, C. C., H. F. Perkins, L. E. Asmussen, and H. D. Allison. 1988a. Using ground-penetrating radar to investigate variability in selected soil properties. Journal of Soil and Water Conservation. 43(4):341-345.

Truman, C. C., H. F. Perkins, L. E. Asmussen, and H. D. Allison. 1988b. Some applications of ground-penetrating radar in the southern coastal plains region of Georgia. The Georgia Agricultural Experiment Stations Research Bulletin No. 362. Univ. of Georgia, Athens. pp. 27.

Williams, B. G. and G. C. Baker. 1982. An electromagnetic induction technique for reconnaissance surveys of soil salinity hazards. Australian J. Soil Res. 20:107-118.

Wollenhaupt, N. C., J. L. Richardson, J. E. Foss, and E. C. Doll. 1986. A rapid method for estimating weighted soil salinity from apparent soil electrical conductivity measured with an aboveground electromagnetic induction meter. Can J. Soil Sci. 66:315-321.



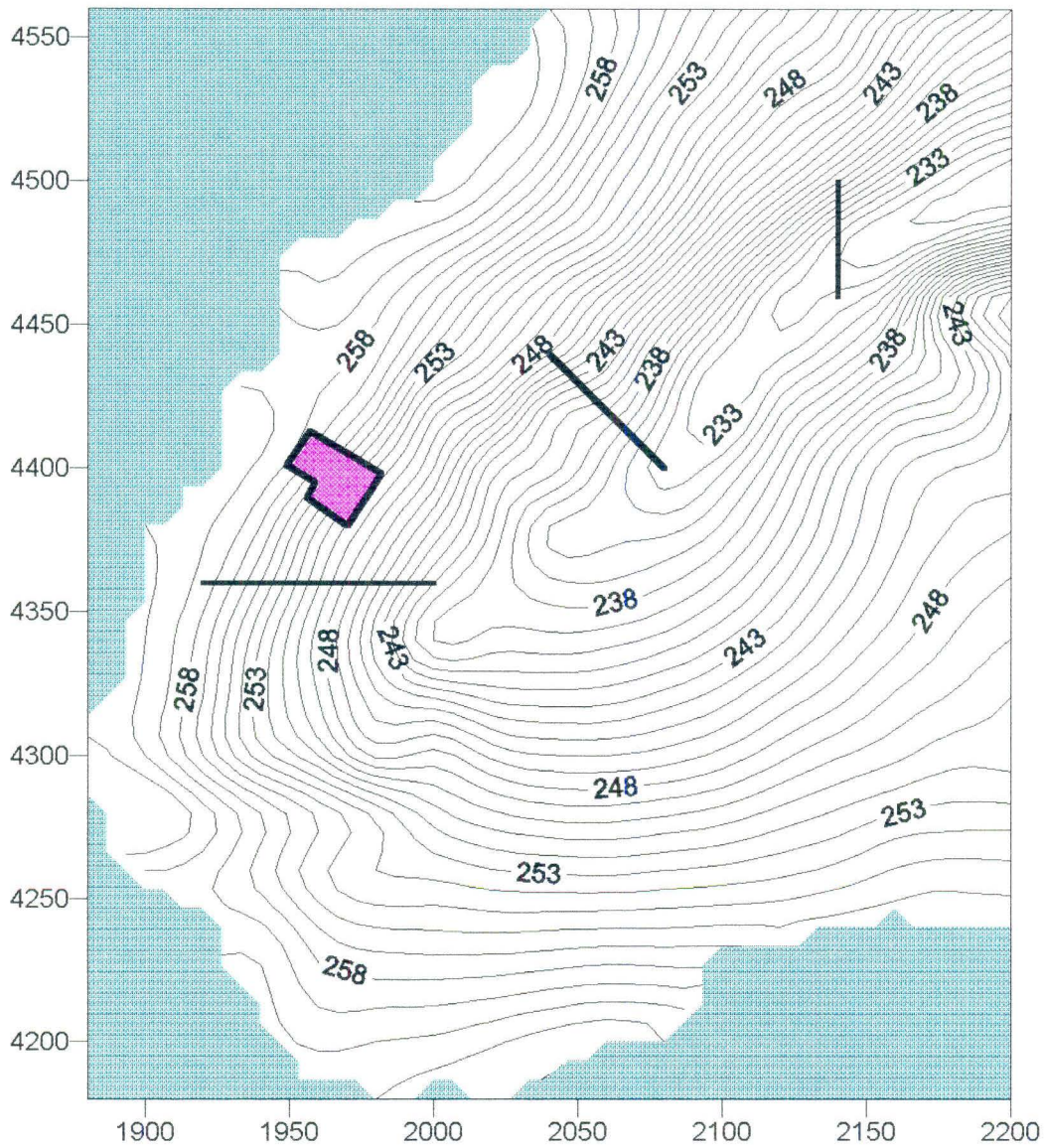
GEORGIA

ATLANTA

■ *Panola Mt. Watershed*

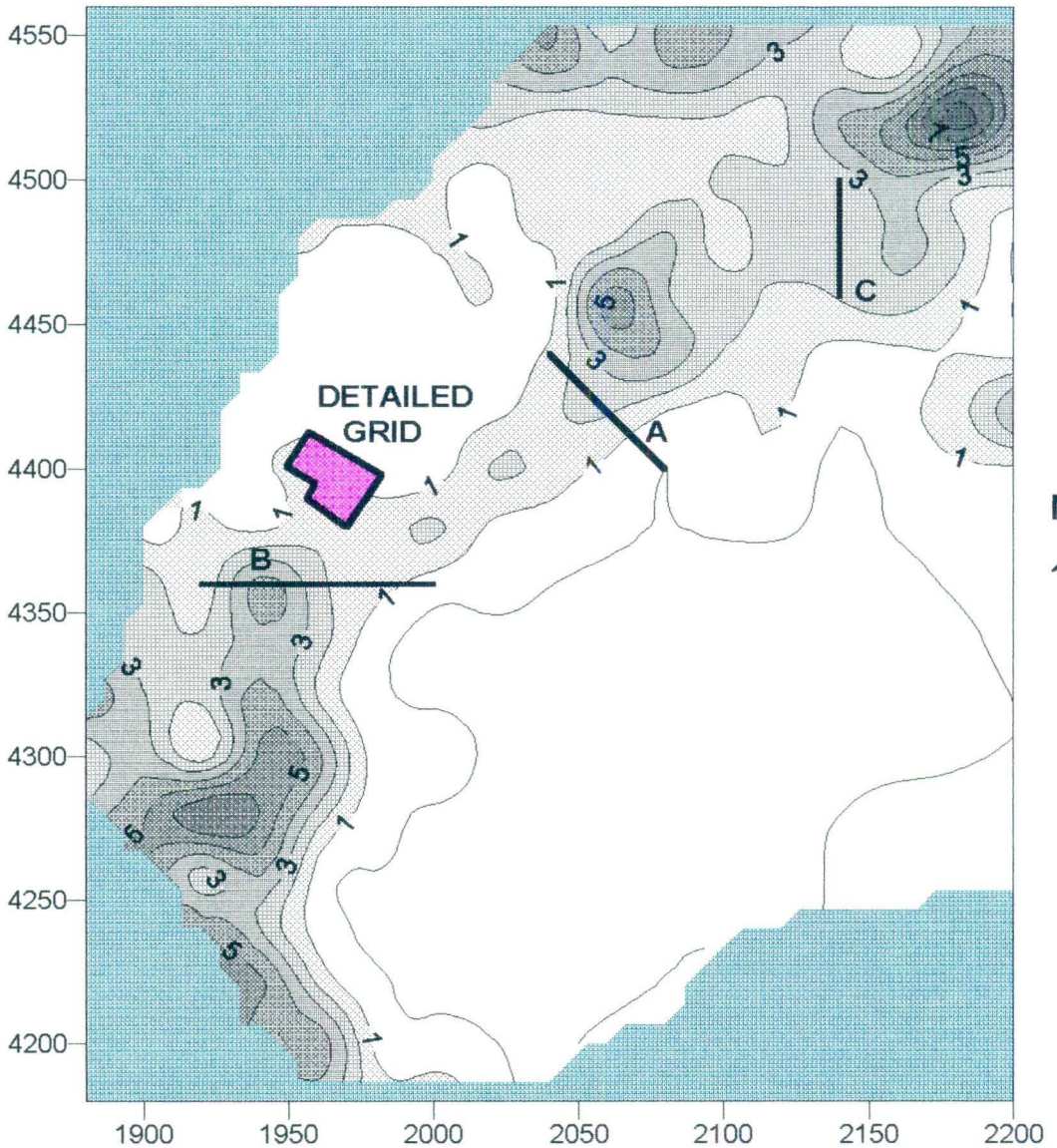
PANOLA MOUNTAIN RESEARCH WATERSHED STOCKBRIDGE, GEORGIA

TOPOGRAPHY



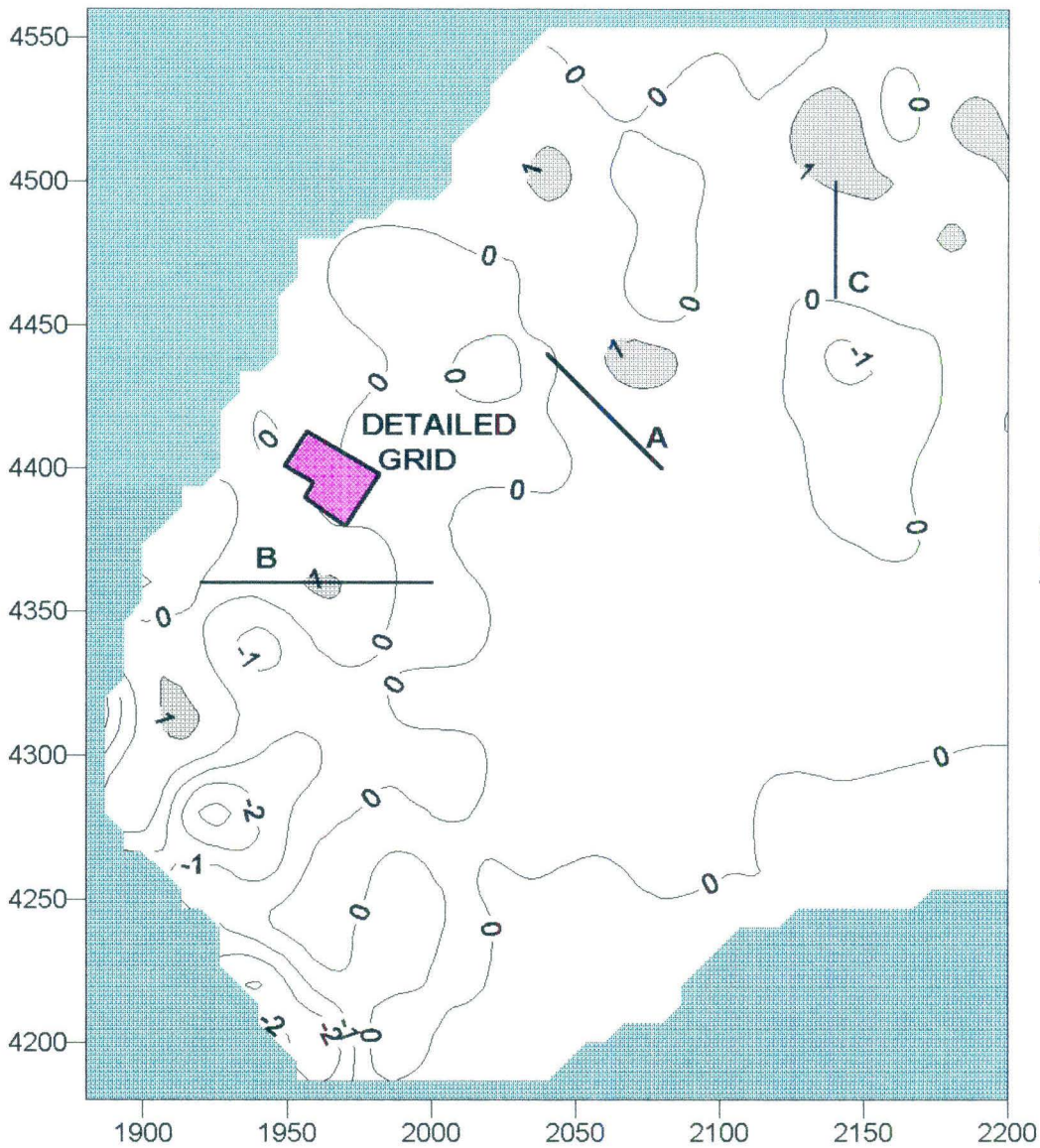
PANOLA MOUNTAIN RESEARCH WATERSHED STOCKBRIDGE, GEORGIA

EM38 SURVEY HORIZONTAL DIPOLE ORIENTATION



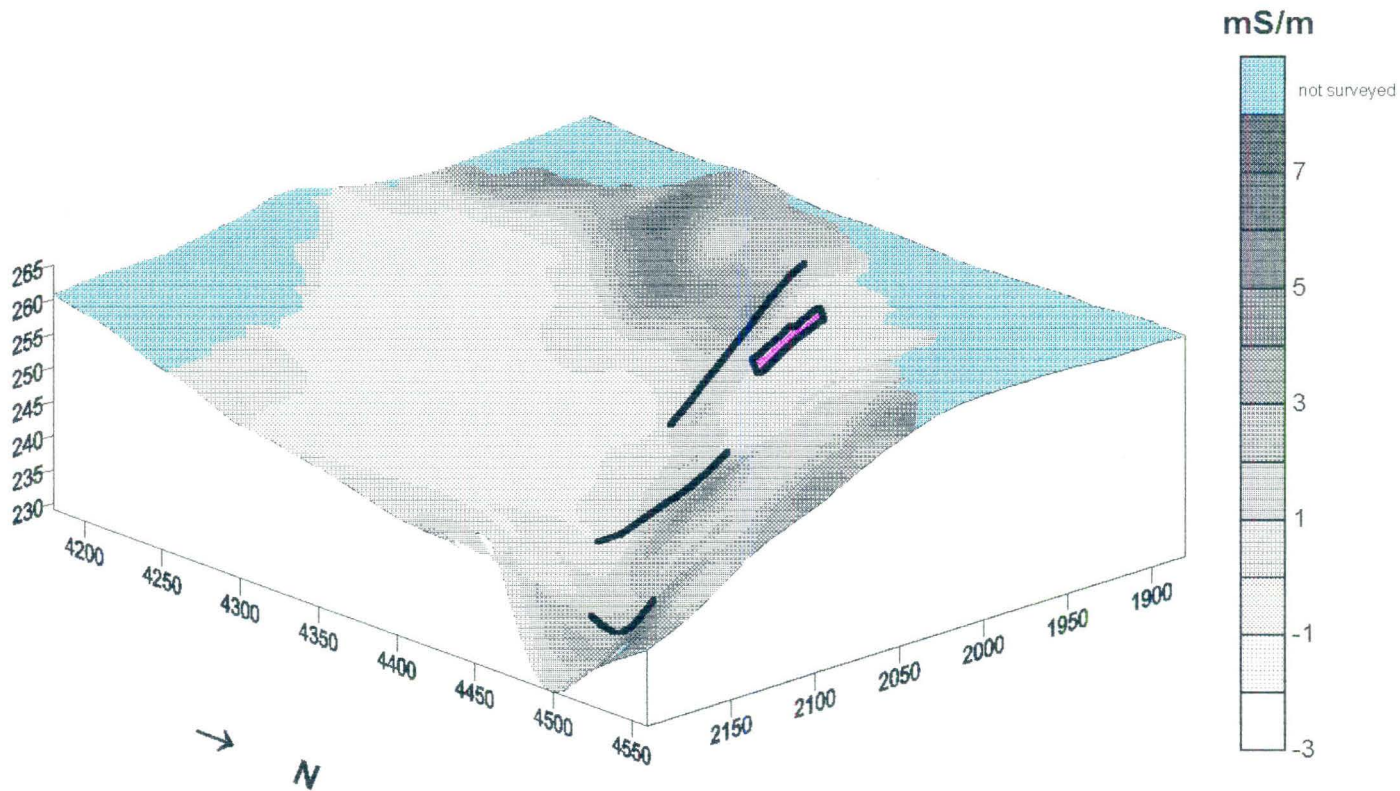
PANOLA MOUNTAIN RESEARCH WATERSHED STOCKBRIDGE, GEORGIA

EM38 SURVEY VERTICAL DIPOLE ORIENTATION



PANOLA MOUNTAIN RESEARCH WATERSHED STOCKBRIDGE, GEORGIA

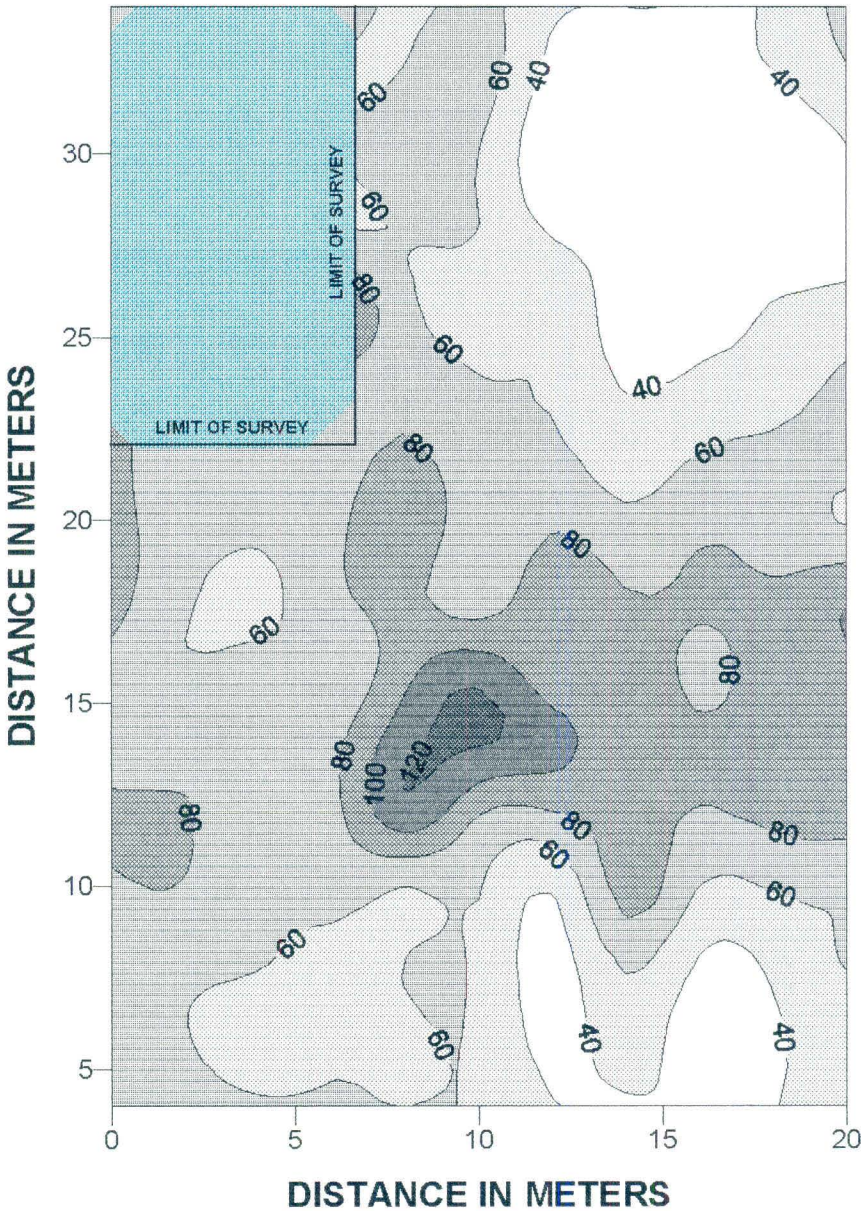
VARIATION IN THE RESPONSE OF
THE EM38 METER (H)
WITH LANDSCAPE POSITION



PANOLA MOUNTAIN RESEARCH WATERSHED STOCKBRIDGE, GEORGIA

GRID SITE

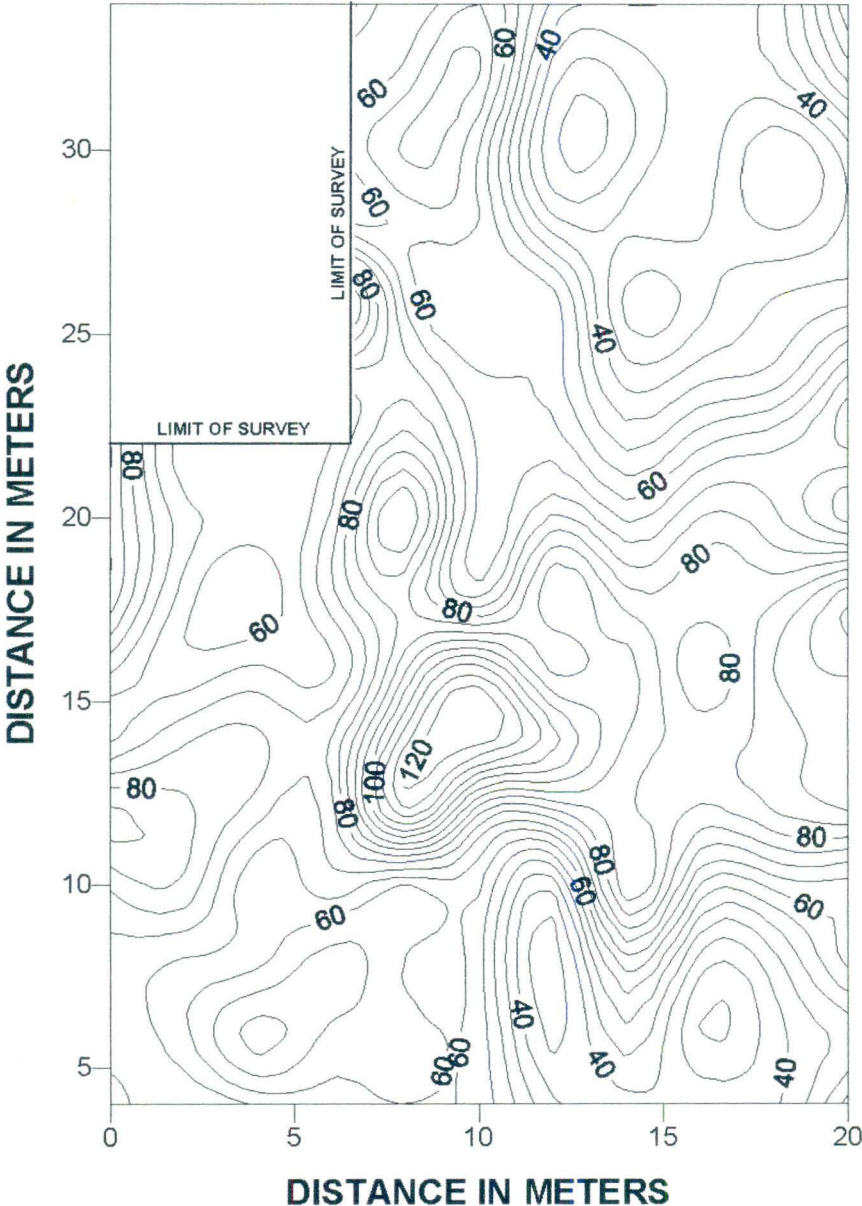
DEPTH TO BEDROCK
CONTOUR INTERVAL = 20 cm



PANOLA MOUNTAIN RESEARCH WATERSHED STOCKBRIDGE, GEORGIA

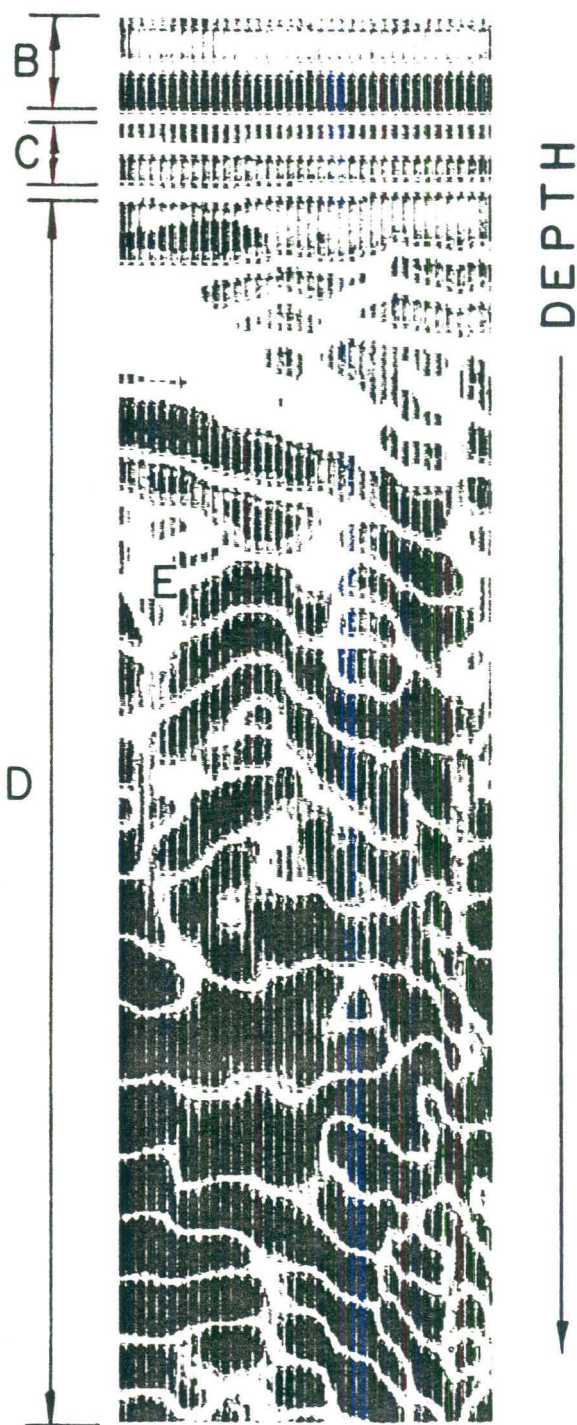
GRID SITE

DEPTH TO BEDROCK
CONTOUR INTERVAL = 5 cm

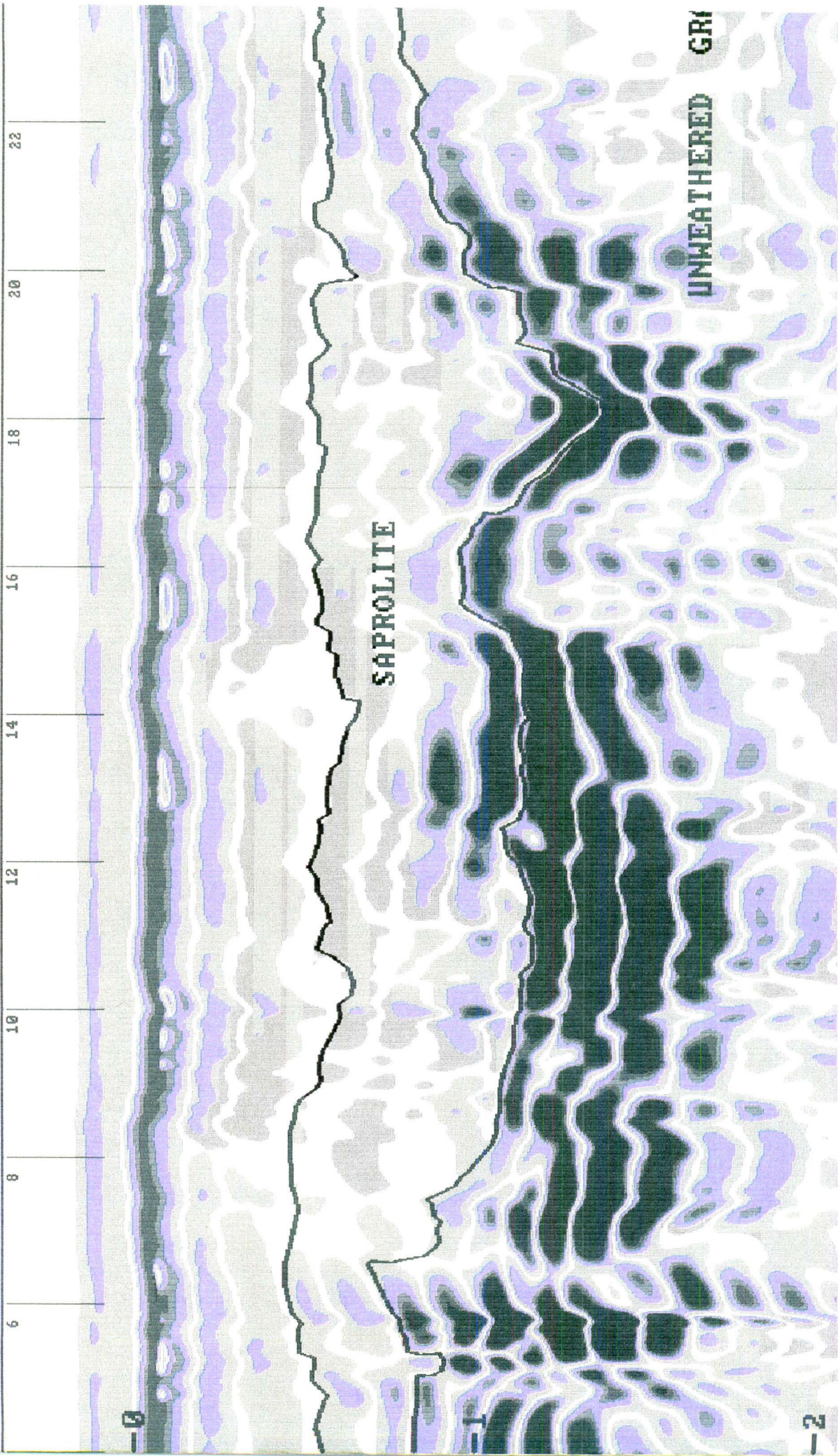


DISTANCE
TRAVELED →

A



RADAR PROFILE



-0

-1

-2

16

18

20

22

24

26

28

30

32

APROLITE

UNWEATHERED GRANITE

